Powder Technology 279 (2015) 86–95

Contents lists available at ScienceDirect

Powder Technology

journal homepage: www.elsevier.com/locate/powtec

Comparative study of two wet chemical methods of $BaSnO_3$ synthesis: Mechanism of formation of mixed oxide

Yasser Halil Ochoa Muñoz [a,*], Miguel Ponce [b], Jorge Enrique Rodríguez Páez [a]

[a] CYTEMAC group—Department of Physics, University of Cauca, Popayán, Colombia
[b] INTEMA, National University of Mar del Plata, Argentina

ARTICLE INFO

Article history:
Received 29 December 2014
Received in revised form 17 March 2015
Accepted 31 March 2015
Available online 7 April 2015

Keywords:
Synthesis
Barium stannate
Controlled precipitation
Pechini
Characterization
Phase evolution

ABSTRACT

Ceramic powders of pure barium stannate ($BaSnO_3$) were synthesized using two wet chemical methods: controlled precipitation and polymeric precursor (Pechini). The obtained ceramic powders were characterized using IR spectroscopy, DTA–TGA, XRD and SEM. Using the precipitation and Pechini methods, single phase $BaSnO_3$ powders were achieved at temperatures of 1250 °C and 1000 °C respectively—substantially lower than the temperatures required for conventional synthesis (>1350 °C). Leading from these results, the physicochemical mechanisms that lead to $BaSnO_3$ formation in the processes of synthesis employed in this work are proposed. This constitutes important information both for determining the advantages and disadvantages of each method and for controlling the characteristics of the powder end product.

1. Introduction

Studies of phase equilibria in the $BaO–SnO_2$ system indicate the existence of two stable phases, $BaSnO_3$ and Ba_2SnO_4 [1] and of another composition phase, $Ba_3Sn_2O_7$ identified at 1400 °C by Appendino and Romanda [2]. $BaSnO_3$ is the most important compound and crystallizes as a perovskite-type, cubic system with a lattice constant value of a 4.1163 Å [3]. There is often difficulty in obtaining pure $BaSnO_3$ because of the formation during synthesis of the Ba_2SnO_4 intermediate.

Ba_2SnO_4 presents a tetragonal K_2NiF_4-type crystal structure, centered in the body, which indicates that $BaSnO_3$ is accommodated non-stoichiometrically in the structure, arranged in alternating layers of perovskite $BaSnO_3$ and rock salt BaO along the c-direction [4]. Formation of Ba_2SnO_4 occurs at ~1200 °C when the precursors $BaCO_3$ and SnO_2 are used. $Ba_3Sn_2O_7$ meanwhile crystallizes in the tetragonal system and structurally comprises perovskite double blocks of $BaSnO_3$ and rock salt BaO along the c-direction [2]; it forms at the higher temperature of ~1400 °C when the same precursors $BaCO_3$ and SnO_2 are used.

Barium stannate, $BaSnO_3$, belongs to the family of alkaline earth stannates ($MSnO_3$, where M = Ca, Sr, Ba) considered n-type semiconductors. $BaSnO_3$ specifically has a band gap value of 3.1 eV [5], well suited to its use as a gas sensor [6]. Studies by Borse et al. [7] and Yuan et al. [8] suggest significant potential for barium stannate systems in photocatalytic applications. Such compounds have been used as a protective coating or catalyst support as a result of their chemical and thermal stability (very high melting point of around 2060 °C [1]). $BaSnO_3$, because of its dielectric properties, has been used to prepare capacitors [9], while $Ba(Ti,Sn)O_3$ solid solutions can be considered as model systems for Pb-free perovskites that show diffuse ferroelectric phase transitions [10].

$BaSnO_3$ ceramic powders are usually obtained by a solid state reaction between $BaCO_3$ and SnO_2 at 1000–1400 °C [11,12]. Other techniques that have been used include hydrothermal [13,14], considering the effect of different solvents [15], sol–gel [16], self-heat-sustained (SHS) route [17], modified combustion [18], and reverse micelle method [19].

Wet chemical synthesis methods constitute an area of substantial research interest specifically because their use offers good control over the physical and chemical characteristics of the solid particles obtained [20]. This ensures that the raw material produced is suited to current technological requirements and guarantees reproducibility in the process and in the characteristics of the end product [21–23]. Synthesis of mixed oxides such as barium stannate brings its difficulties. A common method is to mix barium and tin at the molecular level. This is done using the processes of hydrolysis and condensation of the salts and/or alkoxides of barium and tin. The problem lies in controlling the different rates of hydrolysis and condensation of the tin and barium precursors, i.e. the Sn–OH and Ba–OH functional groups that tend to lead to the formation of clusters, for example of $(Sn–O–Sn)_n$, causing a heterogeneous spatial arrangement of barium and tin. To get around this, researchers

---

* Corresponding author at: Tel.: +57 2 8364243.
E-mail address: yochoa@unicauca.edu.co (Y.H. Ochoa Muñoz).

http://dx.doi.org/10.1016/j.powtec.2015.03.049
0032-5910/© 2015 Published by Elsevier B.V.

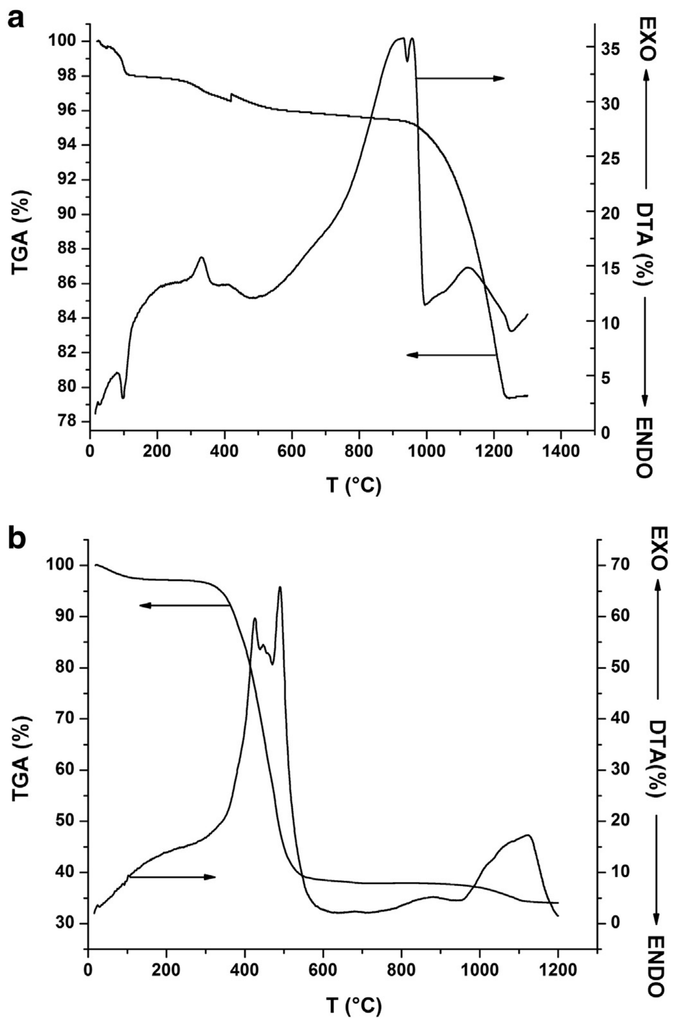

Fig. 1. DTA–TGA curves corresponding to solid samples of the $SnCl_2$–$Ba(CH_3COO)_2$–H_2O–NH_4OH system, synthesized by the controlled precipitation (a) and Pechini (b) methods, heat treated from room temperature to 1300 °C at a rate of 3 °C/min.

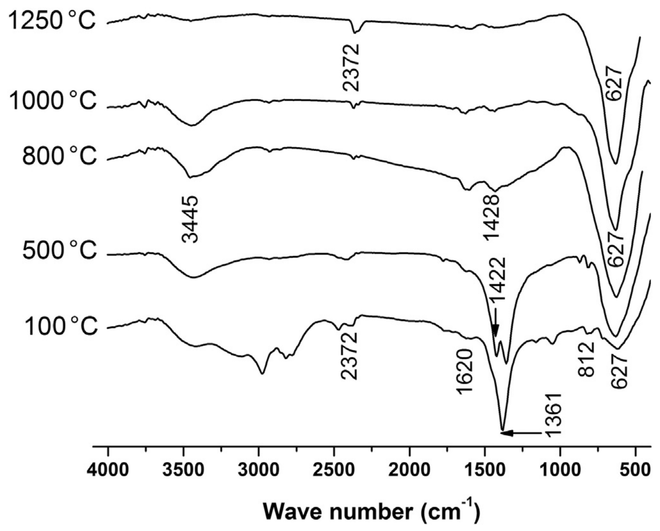

Fig. 2. IR spectra corresponding to solid samples of the $SnCl_2$–$Ba(CH_3COO)_2$–H_2O–NH_4OH system, controlled precipitation method, heat treated at different temperatures.

have been working on a strategy to force the reaction between Sn^{4+} complexes and Ba^{2+} chemical species, to form $BaSnO_3$ directly in solution.

Another option is to break down double salts of the cations of interest, such as oxalates, citrates and/or catecholates [24]. The primary aim of this method is to produce a complex in which tin and barium ions are arranged within it, their links and positions so close together that, on breaking down the complex, barium stannate [20] is formed. The breakdown of such complexes is not simple however. Stable intermediates such as $BaCO_3$ can be formed in the process [25,26]. It is therefore, very important, study both complex formation of Ba–Sn as its decomposition.

Contemplating the double salt strategy, Koferstein et al. [27] modified obtaining the precursor $[Ba(HOC_2H_4OH)_4][Sn(OC_2H_4O)_3]$ for better reproducibility. To do this they used $SnCl_4$, which, through a process of precipitation was obtained ($SnO_2 \cdot nH_2O$). This compound was then used together with $Ba(OH)_2.8H_2O$, to form a slurry in 1,2-ethanediol, at room temperature and in an argon atmosphere. On heating the slurry to 120–130 °C for 8 h, cooling and diluting with propan-2-ol, the barium tin 1,2-ethanediolate complex precursor was obtained. This was then calcined at 820 °C in static air, giving a very fine $BaSnO_3$ with only traces of $BaCO_3$.

Gallagher and Johnson [28] used $BaCO_3$, BaC_2O_4 and SnO_2 to prepare $BaSn(C_2O_4)_2 \cdot 0.5H_2O$ and $Ba_2Sn(C_2O_4)_4 \cdot 6H_2O$ calcined at 800 °C in air to obtain $BaSnO_3$ from the first compound. The study showed that this oxalate compound was decomposed producing $BaCO_3$ and SnO_2. These reacted cleanly and rapidly between 600 and 700 °C to produce $BaSnO_3$ without the formation of intermediate phases such as Ba_2SnO_4.

Pfaff [29] used $BaCl_2$ and $SnCl_4$ as barium and tin precursors and caused them to react with H_2O_2, NH_3 and H_2O to obtain the peroxide $BaSnO_2(O_2) \cdot 3H_2O$. This compound calcined at 900 °C to yield high purity $BaSnO_3$ that featured a large specific surface area and small particle sizes.

Buscaglia et al. [30] meanwhile synthesized the hexahydroxo stannate compound $BaSn(OH)_2$ using $SnCl_4$ and $BaCl_2$ as precursors. These chlorides were dissolved initially in a diluted (0.1 M) aqueous HCl solution that was subsequently poured, with vigorous stirring, into a polypropylene vessel containing a solution of NaOH held at 100 °C in a heat bath. An airstream of purified nitrogen was circulated within the vessel to prevent the formation of carbonates. The $BaSn(OH)_6$ was thermally treated at different temperatures. At between 400 and 700 °C the major crystalline phase was found to be cubic perovskite $BaSnO_3$, with trace amounts of $BaCO_3$. At 1300 °C the mixed oxide was the only crystalline phase present in the solid.

In this article, two synthesis methods used to obtain $BaSnO_3$ are described. In each method, the aim was to be able to exercise control over the process and therefore its reproducibility, in order to guarantee the properties and characteristics desired in the final powder. The ceramic powders obtained were characterized using infrared spectroscopy (IR), X-ray diffraction (XRD) and scanning electron microscopy (SEM). The results of the characterization, together with the study of the formation and evolution of intermediate precursors, allowed a scheme to be structured that gives an idea of the mechanisms involved that lead to the formation of the mixed oxide in each case.

2. Experimental

2.1. Preparation of ceramic powders

2.1.1. Controlled precipitation method

Two aqueous solutions of 0.1 M HNO_3 (Carlo Erba 99%) were prepared independently. The tin precursor, $SnCl_2 \cdot 2H_2O$ (Mallinckrodt 99.6%) was dissolved in one of the solutions and the barium precursor, $Ba(CH_3COO)_2$ (J.T. Baker) in the other. Each solution was stirred constantly at 300 rpm at 50 °C until there were no suspended precursor particles, nor sediment, to be observed. The solutions were then allowed to cool to room temperature. Ammonium hydroxide (NH_4OH-

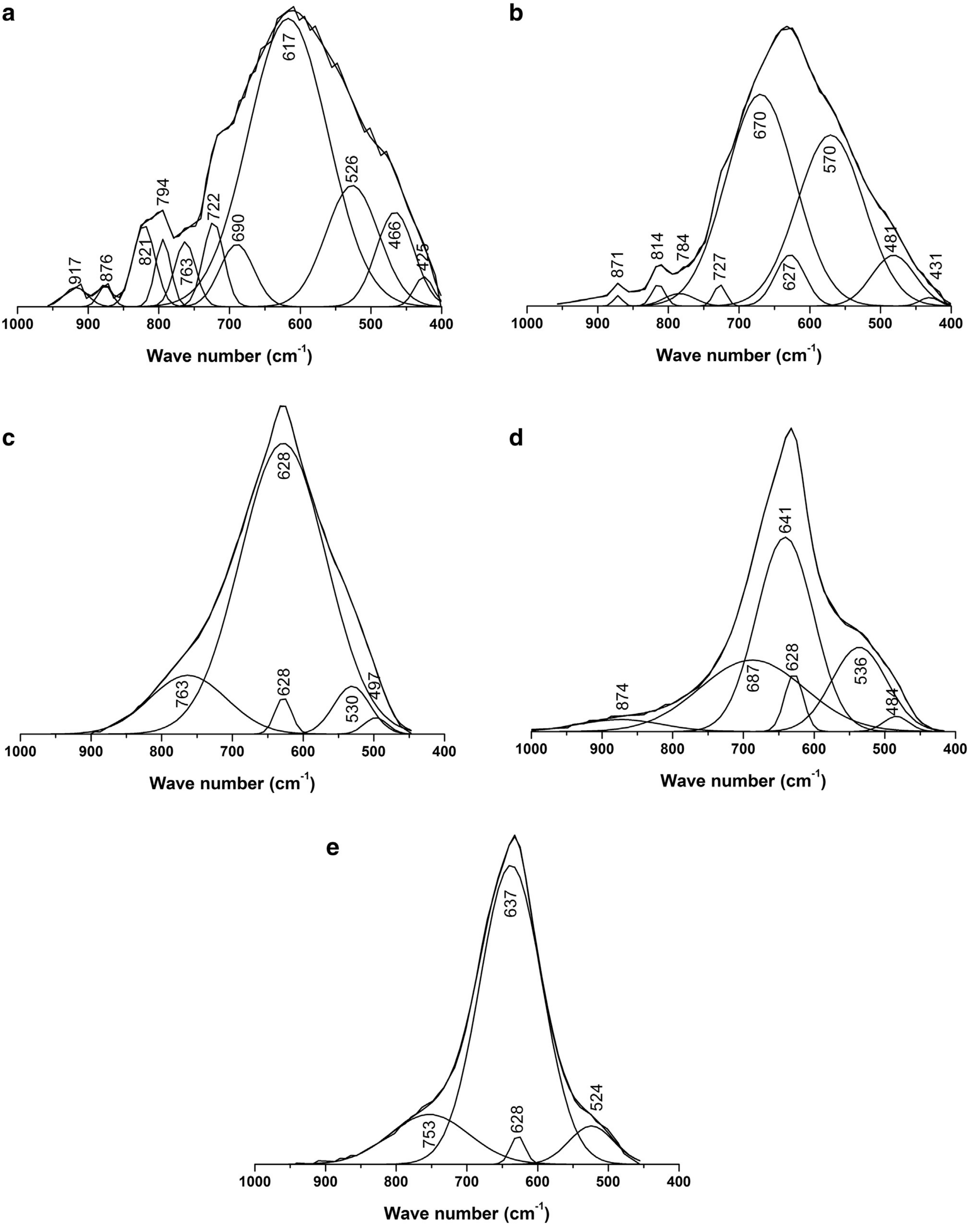

Fig. 3. Deconvolution of IR spectra in the region between 400 and 1000 cm^{-1} corresponding to $SnCl_2$–$Ba(CH_3COO)_2$–H_2O–NH_4OH system solids, controlled precipitation method, heat treated at (a) 100, (b) 500, (c) 800, (d) 1000 and (e) 1250 °C.

Mallincrodt 28%) was then added to each solution at a rate of 0.034 mL/s, using a dispenser (Metrohm Dosimat 685). Variations in the pH of the system were recorded for each solution using a pH meter (Metrohm 744) with a glass electrode. The specific conductivity was measured with a conductivity meter (Toledo model MC126). As NH_4OH was being added, the pH and specific conductivity were simultaneously

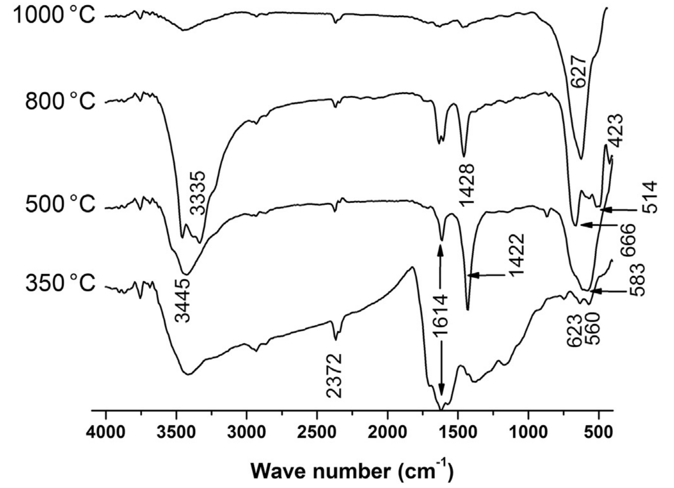

Fig. 4. IR spectra corresponding to solid samples of the $SnCl_2$–$Ba(CH_3COO)_2$–H_2O–NH_4OH system, Pechini method, heat treated at different temperatures.

recorded for the tin and barium systems to plot the data obtained as a function of the volume of NH_4OH precipitant added, obtaining potentiometric and conductimetric titration curves for each system. These curves were used to determine the most suitable pH value that would lead to each solution yielding its respective precipitate. The suspensions obtained were allowed to age for 24 h and then mixed using an Ultraturrax T50. The attempt was made to remove the solvent from the system by vacuum filtering using a Buchi B-169 pump. Too much of the precipitate was lost, however, so it was decided to heat the system to 80 °C in order to volatilize the liquid phase present. The dried solid was macerated in an agate mortar. The powder obtained was then chemically attacked with 0.1 M hydrochloric acid to remove the barium carbonate formed in the samples [31]. Thereafter, the dried solid was ground in an agate mortar and heat treated at a range of temperatures. The powder obtained at the end of this process was the powder characterized.

2.1.2. Polymeric precursor method (Pechini)

In the Pechini method, ethyleneglycol (Mallinckrodt) and citric acid (Merck) were initially mixed at 70 °C to obtain a 4:1 ratio. At room temperature $SnCl_2 \cdot 2H_2O$ and $Ba(CH_3COO)_2$ were added to this ethylene glycol/citric acid solution in quantities determined by the stoichiometry of the mixed oxide desired. Care was taken to ensure that the obtained solution was completely transparent, indicating a uniform mix of the different reagents and favoring citrate formation. NH_4OH was then added to the obtained mixture to bring it to a 9 pH, basic solution, ensuring that no precipitates were formed in the system. Following the addition of the ammonium hydroxide, the system was heat treated at 140 °C

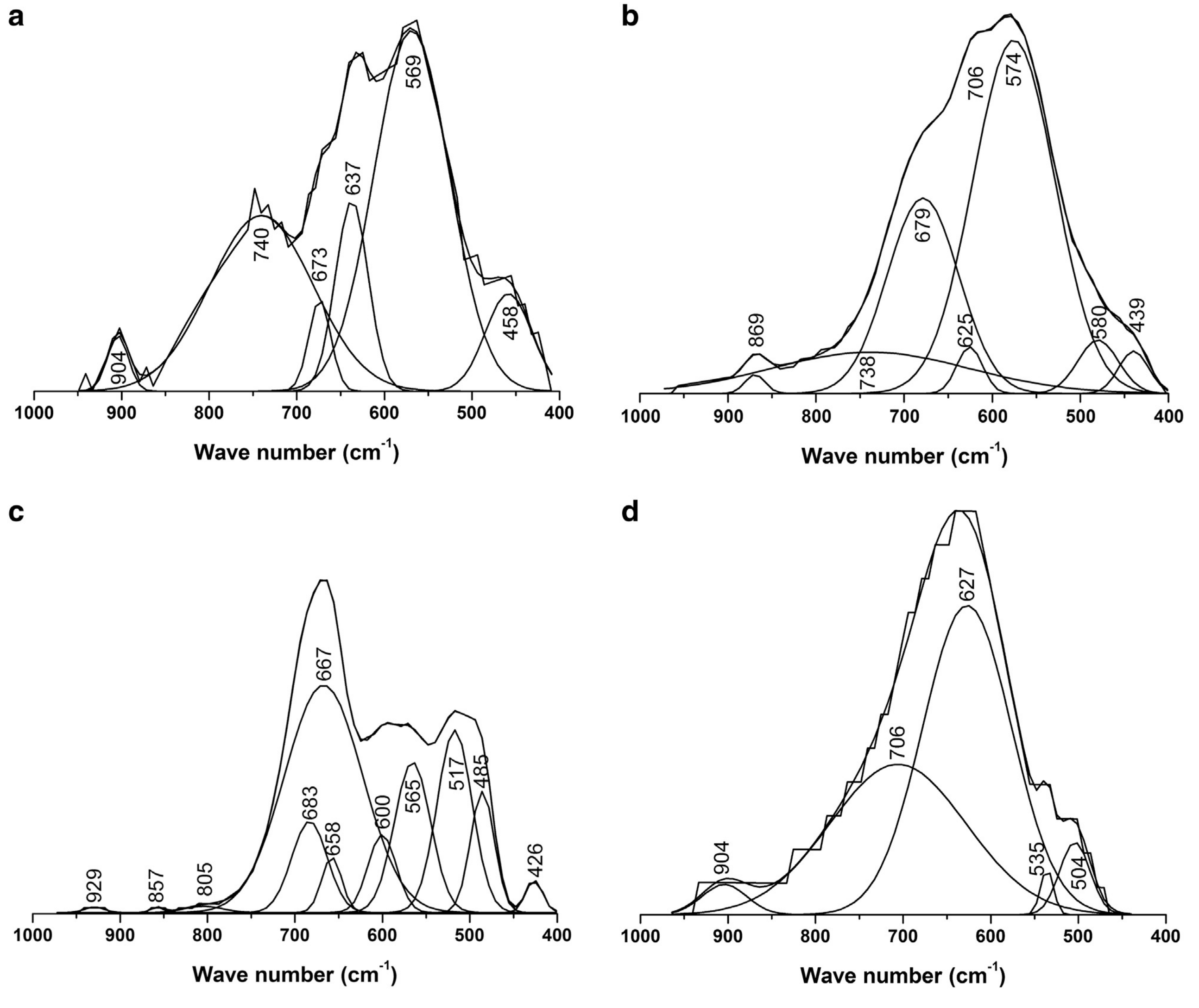

Fig. 5. Deconvolution of IR spectra in the region between 400 and 1000 cm^{-1}, corresponding to solids of the $SnCl_2$–$Ba(CH_3COO)_2$–H_2O–NH_4OH system, Pechini method, heat treated at (a) 350, (b) 500, (c) 900 and (d) 1000 °C.

under continuous stirring to promote polyesterification reactions and the consequent resin formation. The obtained resin was pre-calcined at 350 °C for 2 h to obtain a very fine black solid, with high carbon content. This pre-calcined material was subjected to heat treatments at different temperatures to obtain the $BaSnO_3$.

2.2. Analytical methods

The powders obtained at the end of the synthesis processes were characterized using IR, XRD and SEM (JEOL 5910LV SEM). Thermo Nicolet IR200 equipment was used to obtain the IR spectra and the sample to be analyzed was formed by mixing the synthesized solid with KBr, to obtain the tablet. The X-ray diffractograms were obtained using X TEL-X-OMETER TEL. 580 equipment with a Cu source ($\lambda = 1.54$ Å) and an operating voltage of 30 kV.

3. Results and discussion

3.1. Thermal behavior

To determine the effect of heat treatment on the synthesized particles, thermal analyses were used to look specifically at the effect of temperature on the different stages of transformation of the materials on the way to obtaining the end product desired, analyzing variations in the two chemical methods used.

Fig. 1(a) shows the DTA–TGA curves corresponding to the controlled precipitation powders. The TGA curve initially shows a small weight loss at around 100 °C of ~2%, which may be due to the volatilization of water contained in the sample. This corresponds to the endothermic peak observed at this temperature in the DTA curve. A large weight loss of ~15% is evident between 1000 and 1240 °C and associated with an exothermic peak in the DTA curve at around 1100 °C. This physicochemical event may correspond to the complete formation of the mixed oxide ($BaSnO_3$). Additionally, in the DTA curve, an exothermic peak is observed at ~300 °C and a doublet of very intense peaks between 800 and 1000 °C, possibly associated with the complete decomposition of the barium and tin precursors and the formation of their respective oxides. It could also be associated to the formation of $BaO–SnO_2$ binary system compounds and their decomposition.

The curves in Fig. 1(b) correspond to the results of thermal analysis carried out on the Pechini powders. The TGA curve shows a weight loss of approximately 55% in the range between 350 and 550 °C. In this same temperature region in the DTA curve, several exothermic peaks are observed that could be associated with the formation and decomposition of Sn–Ba organic compounds and to the formation of $BaO–SnO_2$ binary system compounds. Finally, the DTA curve shows a broad exothermic peak between 1000 and 1100 °C, associated with a very small weight loss, which may indicate the complete formation of $BaSnO_3$.

Fig. 1 illustrates the major differences that occur during thermal treatment of the solids obtained in this work using the two synthesis methods—controlled precipitation (Fig. 1(a)) and Pechini (Fig. 1(b))—that led to the formation of $BaSnO_3$.

3.2. Phase evolution during thermal decomposition of Ba and Sn precursors

3.2.1. IR spectroscopy

In order to get information on the evolution of the functional groups during crystallization of the ceramic powder, the dry powders from each synthesis method were characterized using IR spectroscopy. Fig. 2 shows IR spectra corresponding to samples obtained by the controlled precipitation method, heat treated at 100, 500, 800, 1000 and 1250 °C. The results indicate the presence in the solid of hydroxyls, bands around 3445 cm^{-1} showing the presence of absorbed water in the samples, and NO_3^-, a band located at 1361–1395 cm^{-1} [32]. The most evident band is that located at ~630 cm^{-1}, corresponding to a vibrational mode of the Sn–O group of the SnO_3^{2-} (2) [33], and that might be used to demonstrate the existence of $BaSnO_3$. The band at 1422 cm^{-1} is associated with $BaCO_3$ [32,34], so that its intensity decreased at high temperatures. This band appeared in most of the spectra indicating that the $BaCO_3$ was found in the samples as an unwanted additional phase, which required to be removed.

Deconvolution of IR spectrum bands located between 400 and 1000 cm^{-1} (Fig. 2) was carried out in order to use the information on order–disorder phenomena that can occur locally in a solid [35]. Such processes should be important for the formation of the different Ba–Sn intermediate compounds that should lead to obtaining $BaSnO_3$, as indicated in Fig. 1(a). This area of the spectrum was analyzed because it contains the major bands associated with the Sn–O, Sn–C, Ba–O, C–O and Sn–O–Ba functional groups [32–35].

The Fig. 3 spectra demonstrate ongoing re-organization of Ba^{2+} and Sn^{4+} ions on interacting primarily with O^{2-}, CO_3^{-2} and OH^- anions on moving forward the reactions that lead to the formation of the corresponding organic and inorganic compounds. The displacement and the appearance–disappearance of the bands is clearly seen, especially between 100 and 500 °C. Assuming that the band located at ~630 cm^{-1} is characteristic of $BaSnO_3$, it can be concluded that the mixed oxide begins to become apparent in the sample composition from 800 °C.

Fig. 4 shows the IR spectra corresponding to solid samples obtained by the Pechini method, calcined at 350 °C (pre-calcined) and then heat treated at 800 to 1000 °C. The spectra show a band at 3440 cm^{-1} that can be attributed to the vibrational mode of the tension in the H–OH, while the band at 1630 cm^{-1} corresponds to the flexing mode of the water. The band at 1430 cm^{-1} may be associated with the vibration of residual organic C–H groups [32,34]. The band at ~630 cm^{-1} seen in the spectra corresponds to the Sn–O [33]. This band, considered to be characteristic of $BaSnO_3$, is most evident in the treatment at 1000 °C.

Again, the IR spectra (Fig. 4) between 400 and 1000 cm^{-1} were deconvolutioned. The Pechini method results are shown in Fig. 5. As expected, the processes of Ba^{2+} and Sn^{4+} ion re-organization due to reactions occurring within the solid, brought about by the heat treatment undergone by the samples, were very different from those that occurred within the solids obtained by controlled precipitation (Fig. 3), justifying the DTA–TGA results (Fig. 1). For the calcination step, during the Pechini process, the sample is very reactive such that at 900 °C, although the characteristic $BaSnO_3$ band at ~630 cm^{-1} cannot be seen, the presence of this mixed oxide cannot be ruled out since a series of bands appear between 600 and 683 cm^{-1}, indicating that its structure is not yet well ordered locally. In the spectrum of the solid treated at 1000 °C, the band at ~630 cm^{-1} is the most outstanding, stating that the $BaSnO_3$ is an important in the solid phase.

3.2.2. XRD measurements

In Fig. 6, diffractograms corresponding to the controlled precipitation samples indicate that at temperatures below 1000 °C, the samples contain as the main crystalline phase cassiterite, SnO_2 (PDF 77-447), and that by treating them at a higher temperature, specifically at 1250 °C, pure $BaSnO_3$ (PDF 15-780) was obtained. Moreover, at low temperatures, the presence of romarchite, SnO, is evident, which was transformed to SnO_2 as indicated by the diffraction pattern of the solid treated at 500 °C. Additionally, it is interesting to note that while the peaks associated with $BaSnO_3$ are not evident in the X-ray diffraction pattern of the sample treated at 800 °C, the deconvoluted IR spectrum of this sample (Fig. 3(c)) does indicate its presence (band at ~630 cm^{-1}), so that the mixed oxide must either be at a low concentration or still in its amorphous state.

Fig. 7 shows the diffractograms corresponding to solids obtained by the Pechini method, subjected to heat treatment at different temperatures for 2 h. A peak characteristic of $BaCO_3$ is observed in the

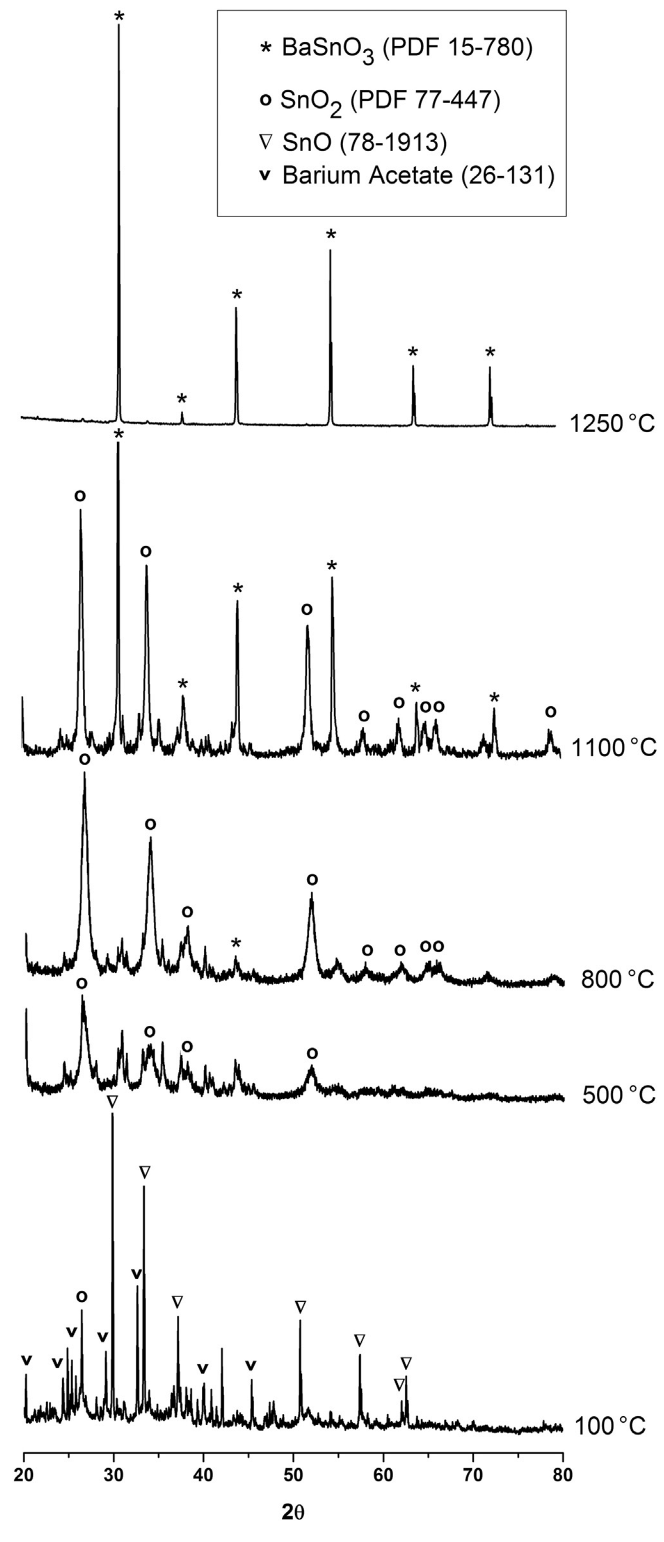

Fig. 6. XRD diffractograms corresponding to solid samples of the Ba–Sn system, controlled precipitation, dried at 100 °C and heat treated at 500, 800, 1100 and 1250 °C for 2 h.

precalcinated sample and $BaSnO_3$ (PDF 15-780) is the principal crystalline phase in the sample treated at 900 °C.

The diffractograms in Figs. 6 and 7 show that for the samples synthesized by the Pechini method, $BaSnO_3$ is obtained at a lower temperature (1000 °C) than for the controlled precipitation samples (1250 °C).

3.2.3. Phase evolution in barium and tin precursors

To consider the process of decomposition of the $BaSnO_3$ precursor during the course of the wet chemical synthesis methods used, it is necessary to indicate how the corresponding precursor would be formed in each case.

3.2.3.1. Controlled precipitation method. Preparation of the intermediate precursor of $BaSnO_3$, using controlled precipitation, was carried out by separately preparing two aqueous solutions containing the corresponding precursors of barium and tin, individually and independently as indicated in the description of the process.

In the case of the slurry containing tin chloride, the indicated method favored the formation of abhurite ($Sn_3O(OH)_2Cl_2$), hydrated tin chloride $SnCl(H_2O)_2SnCl_3(H_2O)$, romarchite (SnO) and cassiterite (SnO_2), as referenced by Ararat et al. [36]. In contrast, in the barium acetate slurry, an aqueous solution acidified with 0.1 M HNO_3, addition of NH_4OH should favor the presence in the system of barium nitrate ($Ba(NO_3)_2$), since the exchange of the NO_3^- ligand for the CH_3OO^- is very efficient, $Ba(NO_3)OH$, NH_4CH_3OO, CH_3COOH, NH_4NO_3 and undissociated $Ba(CH_3COO)_2$ as indicated by Fernández et al. in their work [37]. After allowing these slurries to age, separately, for a day, and then mixing them using a high-shear disperser (Ultraturrax T50), a precipitate containing a heterogeneous mixture of fine particles was obtained, such that the composition of each particle, with respect to the different metal ions and anions present in it, differed from one another.

This co-precipitation process, despite the heterogeneous nature of the precipitate, allowed a solid powder precursor to be obtained on heating the system to 80 °C to volatilize the liquid phase present. This dust would be comprised of fine particles, probably of the order of nanometers. Therefore, the solid sample used for the DTA–TGA curves in Fig. 1(a) would contain primarily a mixture of compounds of the type $Sn_3O(OH)_2Cl_2$, $SnCl(H_2O)_2SnCl_3(H_2O)$, SnO, SnO_2, $Ba(NO_3)_2$, NH_4NO_3 and $BaCO_3$. This latter compound would be produced by the reaction of the Ba^{2+} with the CO_2 in the environment. Attempts were made to remove it by subjecting the synthesized powder to the action of HCl.

Looking again at the curves in Fig. 1(a), the TGA curve initially shows a weight loss of ~2% which should correspond to the release of water from the sample, a process associated with the endothermic peak located at ~100 °C indicated by the DTA curve. Another interesting physicochemical process that occurs in the solid is oxidation of the residual romarchite, shown by a slight increase in the weight of the sample at ~400 °C and associated with the exothermic peaks located between ~320 and ~400 °C, the range within which the romarchite–cassiterite transformation normally occurs [36–38].

Between ~500 and ~1000 °C, Fig. 1(a), a series of events occur that are exothermic in nature, with those at ~900 and ~960 °C standing out. These should correspond to physicochemical processes that generate in the sample a substantial weight loss of around 16%. Particularly notable are those corresponding to the decomposition of the tin and barium compounds mentioned previously, as well as processes with little or no production of volatile compounds; among this latter group must belong the formation and crystallization of $BaSnO_3$, due to the reaction of SnO_2 with the barium compounds present in the solid ($Ba(NO_3)_2$ and $BaCO_3$ for example) through processes of interdiffusion of the constituent ions. As indicated above, the solid powder precursor obtained would mainly contain fine, sub-micron particles. This would cause a reduction in the ion interdiffusion distances compared to the solid state reaction route, leading to shorter reaction times and/or decreased values in the temperature required for the reaction to occur. This behavior of the system is shown in the DTA–TGA curves and corroborated by IR spectroscopy (Figs. 2 and 3) and XRD (Fig. 6). Finally, the broad exothermic peak centered at 1100 °C corresponds to the complete formation and crystallization of $BaSnO_3$. As indicated by XRD results, $BaSnO_3$ formation occurs without the presence of intermediate stages such as Ba_2SnO_4.

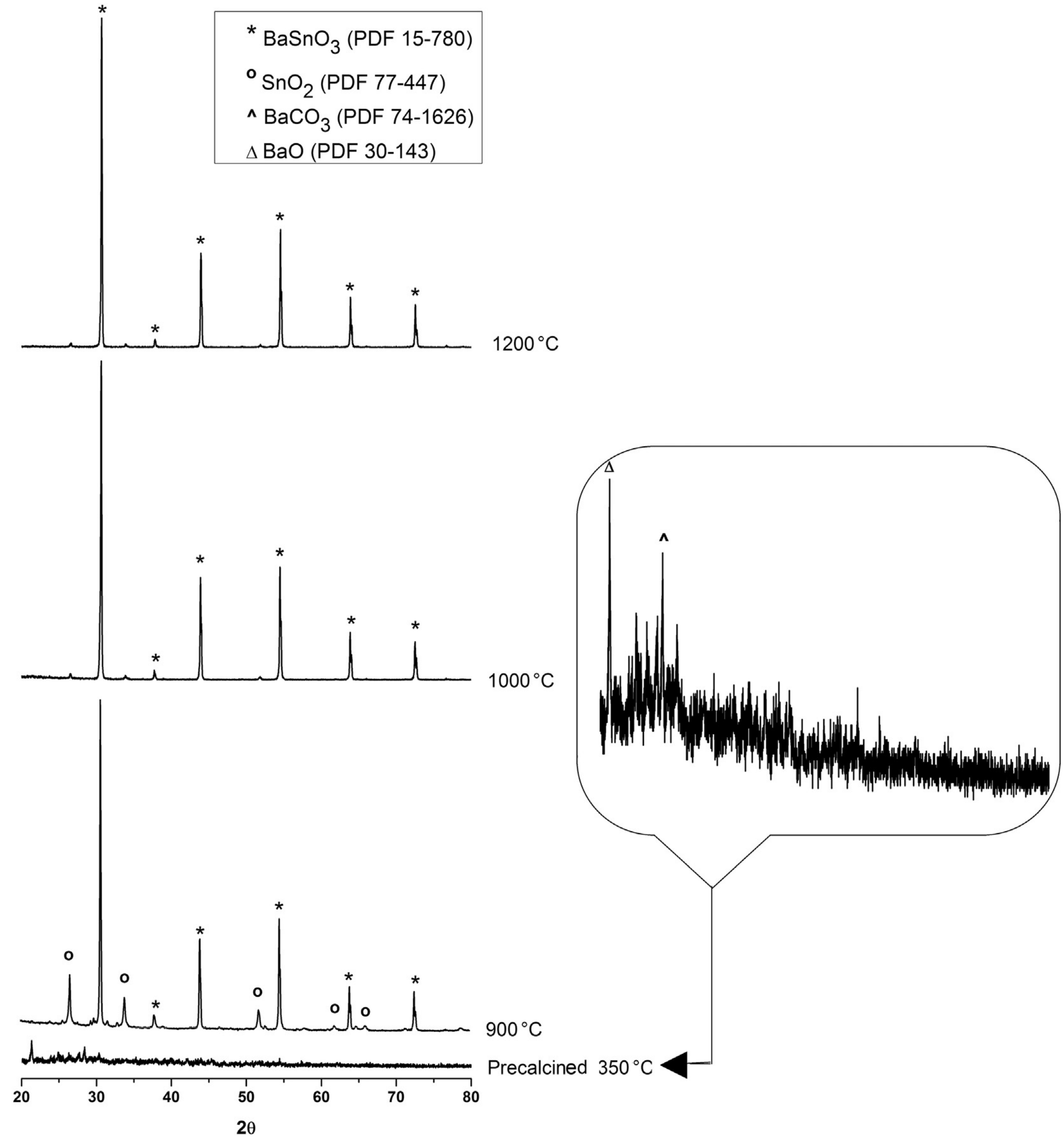

Fig. 7. XRD diffractograms corresponding to solid samples of the Ba–Sn system, Pechini method, treated at different temperatures.

3.2.3.2. Pechini method. In the first step, citric acid (CA) is dissolved in ethyleneglycol (EG) at a temperature of 70 °C, promoting the following reactions [20]:

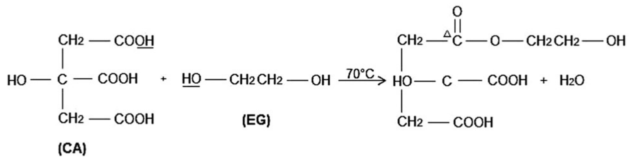

$$\begin{array}{c}\mathrm{CH_2-CO\underline{OH}}\\ |\\ \mathrm{HO-C-COOH}\\ |\\ \mathrm{CH_2-COOH}\\ \mathbf{(CA)}\end{array} + \underset{\mathbf{(EG)}}{\mathrm{\underline{HO}-CH_2CH_2-OH}} \xrightarrow{70^\circ C} \begin{array}{c}\mathrm{CH_2\overset{\triangle}{-}\overset{O}{\overset{\|}{C}}-O-CH_2CH_2-OH}\\ |\\ \mathrm{HO-C-COOH}\\ |\\ \mathrm{CH_2-COOH}\end{array} + \mathrm{H_2O} \qquad (1)$$

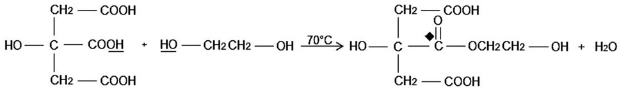

$$\begin{array}{c}\mathrm{CH_2-COOH}\\ |\\ \mathrm{HO-C-CO\underline{OH}}\\ |\\ \mathrm{CH_2-COOH}\end{array} + \mathrm{\underline{HO}-CH_2CH_2-OH} \xrightarrow{70^\circ C} \begin{array}{c}\mathrm{CH_2-COOH}\\ |\\ \mathrm{HO-C\overset{\blacklozenge}{-}\overset{O}{\overset{\|}{C}}-OCH_2CH_2-OH}\\ |\\ \mathrm{CH_2-COOH}\end{array} + \mathrm{H_2O} \qquad (2)$$

as widely discussed by Kakihana [20].

After cooling the CA–EG solution, the precursors of barium (barium acetate) and tin (stannous chloride) are added and the mixture was subjected to a heat treatment at 140 °C. This would particularly promote the following reactions:

(a) Esterification of the citric acid with the ethyleneglycol [20,39]

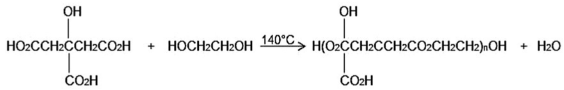

$$\mathrm{HO_2CCH_2\overset{\overset{OH}{|}}{\underset{\underset{CO_2H}{|}}{C}}CH_2CO_2H} + \mathrm{HOCH_2CH_2OH} \xrightarrow{140^\circ C} \mathrm{H(O_2\overset{\overset{OH}{|}}{\underset{\underset{CO_2H}{|}}{C}}CH_2CCH_2CO_2CH_2CH_2)_nOH} + \mathrm{H_2O} \qquad (3)$$

(b) Chelation of the barium acetate

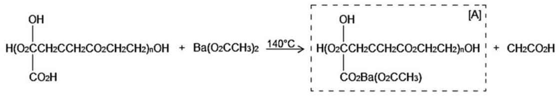

$$\mathrm{H(O_2\overset{\overset{OH}{|}}{\underset{\underset{CO_2H}{|}}{C}}CH_2CCH_2CO_2CH_2CH_2)_nOH} + \mathrm{Ba(O_2CCH_3)_2} \xrightarrow{140^\circ C} \boxed{\mathrm{H(O_2\overset{\overset{OH}{|}}{\underset{\underset{CO_2Ba(O_2CCH_3)}{|}}{C}}CH_2CCH_2CO_2CH_2CH_2)_nOH}\ ^{[A]}} + \mathrm{CH_2CO_2H} \qquad (4)$$

(c) Chelation of the tin chloride

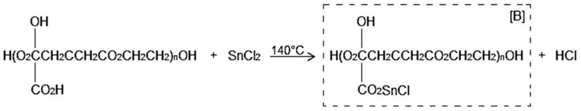

$$H(O_2CCH_2\overset{OH}{\underset{CO_2H}{C}}CH_2CO_2CH_2CH_2)_nOH + SnCl_2 \xrightarrow{140^\circ C} \boxed{H(O_2CCH_2\overset{OH}{\underset{CO_2SnCl}{C}}CH_2CO_2CH_2CH_2)_nOH}^{[B]} + HCl \quad (5)$$

Other reactions that may occur during this heat treatment at 140 °C would lead to the formation of barium–tin–ammonium citrate complexes stabilized in EG, which would be formed on addition of NH_4OH to the original mixture (Ba and Sn–CA–EG precursors) to adjust the working pH (a basic pH), barium–tin glycolates (BTG), for example $BaSn(C_2H_4O_2)_3 \cdot 4C_2H_6O_2 \cdot H_2O$ and $[Ba(C_2H_6O_2)_4][Sn(C_2H_4O_2)_3]$ [25–27], and barium–tin citrates (for example $BaSn(C_6H_6O_7)_3 \cdot nH_2O$), complexes whose formation is favored if reactions (1) and (2) do not fully carry through, with the CA and EG remaining unreacted and/or by the evaporation of EG.

The prolonged heating of the original mixture at 140 °C for 5 h would promote the esterification reaction (Eq. (3)) and the formation of stable Ba–Sn chelate complexes (Eqs. (4) and (5)) such as Ba–Sn–CA complexes; as indicated by Kakihana [20], many of these Ba–Sn citrate complexes may be soluble and stable in EG and water. The theoretical calculations, meanwhile, of Tai and Lessing [40] indicate that the critical composition of the EG/AC mixture in order to favor gelation is 60/40 (mole ratio). This calculation is based on the assumption that simplified polyesterification between CA and EG occurs. This critical composition differs considerably from that used in this work, EG/CA = 80/20 and proposed in the original patent of Pechini [41], so that the esterification of the CA, both free and complexed, would occur in the presence of EG; an excess of EG would act as a solvent increasing the solubility of the various metal salts in the early stages of the process.

During the 5 h of heat treatment at 140 °C to which the original mixture is subjected, the progress of the reactions listed above is favored. These would be accompanied by the evaporation of excess EG, promoting esterification and as such a transparent polymeric resin would be obtained, as was the case. Given the high thermal stability of the Ba–Sn citrates at the working temperature (140 °C) [20], they ought to remain frozen in a polymer network, maintaining the initial stoichiometric ratio of the barium and tin cations. This polymeric resin would be expected to contain randomly branched polymer molecules, throughout which the cations are uniformly available as shown in Fig. 8, where "A" and "B" represent the complexes indicated in reactions 4 and 5.

On calcining the polymeric resin at 350 °C for 2 h, a breakdown of the polymer would be promoted and since Ba–Sn acetate complexes ought to predominate in the resin, it is expected that these compounds thermally decompose in a way that is analogous to other systems [42,43], by way of the following reaction types:

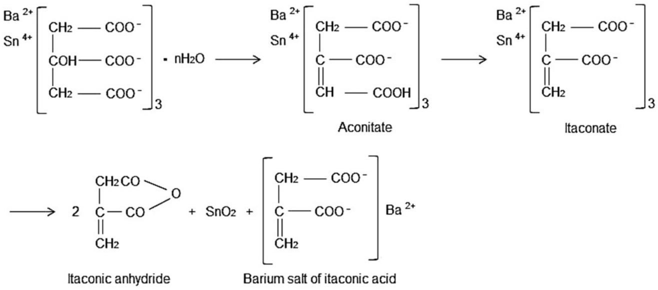

These reactions take place during the heat treatment undergone by the resin—from room temperature to 350 °C and then maintaining this temperature for 2 h. It is therefore expected that the pre-calcined black-colored sample used for the DTA–TGA curves (Fig. 1(b)), may contain mainly Ba–Sn itaconate, itaconic anhydride, amorphous oxide of tin and barium salts of itaconic acid, since barium is more basic than tin.

Fig. 1(b) shows the manner of the thermal decomposition of the precursor of $BaSnO_3$, a solid compound that would contain the compounds mentioned above. The DTA–TGA curves obtained for this precursor show a substantial weight loss, with three major exothermic events in the range between ~330 and ~540 °C. The exothermic peaks between ~420 and ~500 °C could be associated mainly to the complete decomposition of the double Ba–Sn carboxylic salt (Ba–Sn itaconate) and the combustion of itaconic anhydride in air. The exothermic peak at ~530 °C should provide information on the decomposition of the barium salt of itaconic acid and the crystallization of the amorphous SnO_2 that should exist in the sample, considering the proposed reactions. Between ~750 and 900 °C, Fig. 1(b), a small, wide exothermic peak is observed which should give information about the crystallization of the $BaSnO_3$, coinciding with that enunciated by Koferstein in his work [26]. Finally, between ~950 and ~1200 °C there is a quite obvious exothermic peak indicating the complete formation and crystallization of $BaSnO_3$.

The DTA–TGA curves in Fig. 1 differ according to the synthesis method used to obtain the $BaSnO_3$. On one hand there would be the reaction between particles of different composition which form a heterogeneous physical mixture of materials in bulk, Fig. 1(a); on the other the

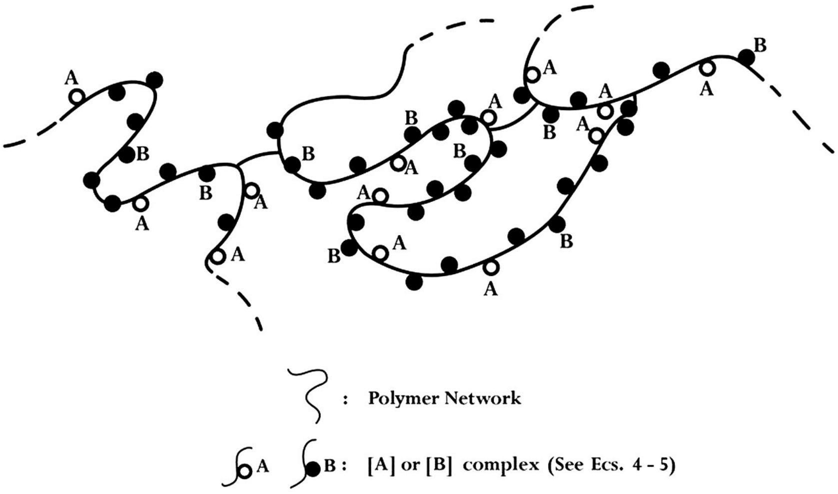

Fig. 8. Diagram showing resin formation during the Pechini [20] process.

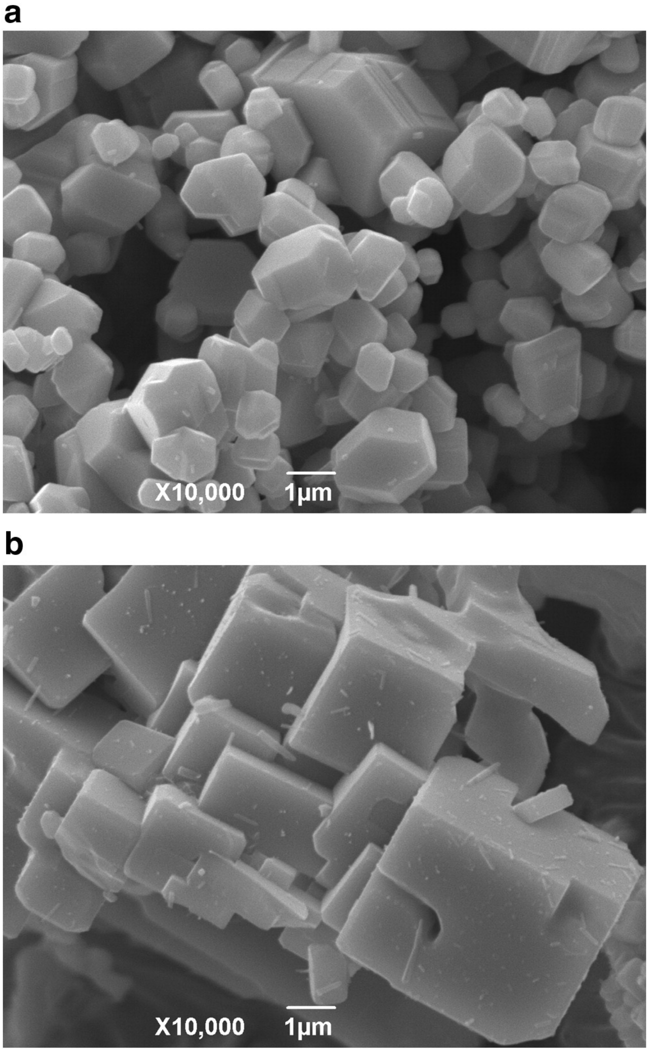

Fig. 9. SEM photographs of powders of $BaSnO_3$ synthesized by: (a) controlled precipitation, at 1250 °C and (b) Pechini, at 1000 °C.

decomposition of double salts (Fig. 1(b)), mainly citrates as shown in the proposed reactions. In cases where the physical mixture of the bulk material is made up of coarser particles, these are not intimately mixed. Reactions between these particles can be described using geometrical rate laws and are slow, also requiring certain diffusion paths. These characteristics of the synthesis process cause $BaSnO_3$ to form at high temperatures, in this case above 800 °C, the only crystalline phase being at 1250 °C (see Figs. 3 and 6). Furthermore, decomposition of the double salts (especially citrates) generates a highly reactive intimate mixture of compounds of Ba^{2+} and Sn^{4+} (Eqs. (4) and (5)) that favors the formation of $BaSnO_3$ as the main crystalline phase at a relatively low temperature, ~1000 °C (see Figs. 5 and 7).

3.2.4. Electron microscopy

Fig. 9 shows SEM micrographs of ceramic powders of $BaSnO_3$ heat treated at 1250 °C, obtained by the controlled precipitation method (Fig. 9(a)), and at 1000 °C, for those synthesized by the Pechini method (Fig. 9(b)). The presence of agglomerates larger than 1 μm, with polyhedral shapes (controlled precipitation) and larger than 5 μm, with cubic shapes (Pechini) can be observed.

4. Conclusions

Using the synthesis methods proposed in this paper, controlled precipitation and polymeric precursor (Pechini), $BaSnO_3$ powders could be prepared in a controlled, reproducible way. The XRD results showed that solids obtained by controlled precipitation and Pechini were found as the pure crystalline phase of $BaSnO_3$ of interest when treated at 1250 and 1000 °C respectively.

In the IR spectra corresponding to these samples, meanwhile, a band located between 618 and 630 cm^{-1} was evident, associated with a vibrational mode of the Sn–O group in the SnO_3^{2-}, which could be used to demonstrate the existence of $BaSnO_3$. The heat treatment to which the samples were subjected favored the formation of agglomerates with a size of <1 μm for those synthesized by controlled precipitation and <5 μm for those obtained by the Pechini method. In the article, mechanisms are proposed that make it possible to explain how the mixed oxide particles form, taking account of chemical reactions that could occur as the process continued and that would be favored by the heat treatment.

Acknowledgments

We are grateful to the VRI of the University of Cauca for funding project ID 3587 and for providing logistical support. We are especially grateful to Colin McLachlan for suggestions relating to the English text.

References

[1] V.G. Wagner, H. Binder, Undersuchung der binären system BaO–SnO_2 und BaO–PbO_2. II Kristallstrukturbestimmungen, Z. Anorg. Allg. Chem. 298 (1959) 12–21.
[2] P. Appendino, G. Ramonda, Equilibri allo stato solido nel sistema ossido di barrio-ossido di stronzio-biossido di stagno, Ann. Chim. (Rome) 61 (1971) 54–60.
[3] V. Vorgelegt, L. Wensheng, Synthesis of nanosized $BaSnO_3$ powdersDoctoral thesis in Engineering of Natural Sciences, Faculty of Engineering, University of Saarlandes, Saarbrücken—Germany 2002. 1–2.
[4] V.G. Wagner, H. Binder, Untersuchung der binärin systeme BaO–SnO_2 und BaO–PbO_2. I Phasenanalysen, Z. Allg. Anorg. Chem. 297 (1958) 328–346.
[5] W. Zhang, J. Tang, J. Ye, Structural, photocatalytic, and photophysical properties of perovskite $MSnO_3$ (M = Ca, Sr and Ba) photocatalysts, J. Mater. Res. 22 (7) (2007) 1859–1871.
[6] J. Cerda, J. Arbiol, G. Dezanneau, R. Díaz, J.R. Morante, Perovskite-type $BaSnO_3$ powders for high temperature gas sensor applications, Sensors Actuators B 84 (2002) 21–25.
[7] P.H. Borse, J.S. Lee, H.G. Kim, Theoretical band energetic of $Ba(M_{0.5}Sn_{0.5})O_3$ for solar photoactive applications, J. Appl. Phys. 100 (2006) 124915.
[8] Y. Yuan, J. Lv, X. Jiang, Large impact of strontium substitution on photocatalytic water splitting activity of $BaSnO_3$, Appl. Phys. Lett. 91 (2007) 094107.
[9] Z. Zhigang, Z. Gang, BTS: a new ferroelectric for multifunctional sensors, Ferroelectrics 101 (1990) 43–54.
[10] G.A. Smolensky, Physical phenomena in ferroelectrics with diffused phase transition, Proceeding of the second International Meeting of Ferroelectrics or Journal of the Physical Society of Japan, 28 1970, p. 26 (supplement).
[11] T. Huang, T. Nakamura, M. Itoh, Y. Inaguma, O. Ishiyama, Electrical properties of $BaSnO_3$ in substitution of antimony for tin and lanthanum for barium, J. Mater. Sci. 30 (1995) 1556–1560.
[12] S. Upadhyay, O. Parkash, D. Kumar, Solubility of lanthanum, nickel and chromium in barium stannate, Mater. Lett. 49 (2001) 251–255.
[13] W. Lu, H. Schmidt, Hydrothermal synthesis of nanocrystalline BaSnO3 using a $SnO_2.xH_2O$ sol, J. Eur. Ceram. Soc. 25 (2005) 919–925.
[14] W. Lu, H. Schmidt, Synthesis of tin oxide hydrate ($SnO_2.xH_2O$) gel and its effects on the hydrothermal preparation of $BaSnO_3$ powders, Adv. Powder Technol. 19 (2008) 1–12.
[15] W. Lu, H. Schmidt, Lyothermal synthesis of nanocrystalline BaSnO3 powders, Ceram. Int. 34 (2008) 645–649.
[16] W. Lu, H. Schmidt, Synthesis of nanosized $BaSnO_3$ powders from metal isopropoxides, J. Sol-Gel Sci. Technol. 42 (2007) 55–64.
[17] A.M. Azad, L.W. Shyan, T.Y. Pang, C.H. Nee, Microstructural evolution in $MSnO_3$ ceramics derived via self-heat-sustained (SHS) reaction technique, Ceram. Int. 26 (2000) 685–692.
[18] A.S. Deep, S. Vidya, P.C. Manu, S. Solomon, A. John, J.K. Thomas, Structural and optical characterization of $BaSnO_3$ nanopowder synthesized through novel combustion technique, J. Alloys Compd. 509 (2011) 1830–1835.
[19] J. Ahmed, C.K. Blakely, S.R. Bruno, V.V. Poltavets, Synthesis of $MSnO_3$ (M = Ba, Sr) nanoparticles by reverse micelle method and particle size distribution analysis by whole powder pattern modeling, Mater. Res. Bull. 47 (2012) 2282–2287.
[20] M. Kakihana, “Sol–gel” preparation of high temperature superconducting oxides, J. Sol-Gel Sci. Technol. 6 (1996) 7–55.

[21] D. Ganguli, M. Chatterjee, Ceramic Powder Preparation: A Handbook, Kluwer Academic Publishers, Massachusetts, 1997.

[22] F. Bensebaa, Nanoparticle Technologies: From Lab to Market, Elsevier Ltd, San Diego, 2013.

[23] K. Lu, Nanoparticulate Materials: Synthesis, Characterization and Processing, John Wiley & Sons, Inc, New Jersey, 2013.

[24] J.A. Davis, S. Dutremez, Electroceramics from source materials via molecular intermediates: $BaTiO_3$ from TiO_2 via (Ti(catecholate)3)$^{-2}$, J. Am. Ceram. Soc. 73 (5) (1990) 1429–1430.

[25] L. Jäger, V. Lorenz, T. Müller, H.P. Abicht, M. Rössel, H. Görls, Barium stannate powders from hydrothermal synthesis and by thermolysis of barium-Tin(IV)-glycolates. Synthesis and structure of $[Ba(C_2H_6O_2)_4][Sn(C_2H_4O_2)_3]$ and $[Ba(C_2H_6O_2)_2][Sn(C_2H_4O_2)_3].CH_3OH$, Z. Anorg. Allg. Chem. 630 (2004) 189–195.

[26] R. Köferstein, H.P. Abicht, J. Woltersdorf, E. Pippel, Phase evolution of a barium tin 1,2-ethanediolato complex to barium stannate during thermal decomposition, Thermochim. Acta 441 (2006) 176–183.

[27] R. Köferstein, L. Jäger, M. Zenkner, S.G. Ebbinghaus, Nano-sized $BaSnO_3$ powder via a precursor route: comparative study of sintering behavior and mechanism of fine and coarse-grained powders, J. Eur. Ceram. Soc. 29 (2009) 2317–2324.

[28] P.K. Gallagher, D.W. Johnson Jr., Kinetics of the formation of $BaSnO_3$ from barium carbonate and tin (IV) oxide or oxalate precursors, Thermochim. Acta 4 (1972) 283–289.

[29] G. Pfaff, Wet chemical synthesis of $BaSnO_3$ and Ba_2SnO_4 powders, J. Eur. Ceram. Soc. 12 (1993) 159–164.

[30] M.T. Buscaglia, M. Leoni, M. Viviani, V. Buscaglia, A. Martinell, A. Testino, P. Nanni, Synthesis and characterization of $BaSn(OH)_6$ and $BaSnO_3$ acicular particles, J. Mater. Res. 18 (3) (2003) 560–566.

[31] C. Fernández Perdomo, E. Rivera Figueroa, J.E. Rodríguez-Páez, $BaTiO_3$ cubic synthesis by chemical ways, Rev. Fac. Ing. Univ. Antioquia 56 (2010) 9–19.

[32] G. Socrates, Infrared and Raman Characteristic Group Frequencies: Tables and Charts, Third edition John Wiley & Sons Ltd., West Sussex, 2001.

[33] D. Amalric–Popescu, F. Bozon–Verduraz, Infrared studies on SnO_2 and Pd/SnO_2, Catal. Today 70 (2001) 139–154.

[34] K. Nakamato, “Infrared and Raman spectra of inorganic and coordination compounds”, part A, B, Fifth edition John Wiley & Sons Inc., New York, 1997.

[35] W.B. White, Order–disorder effectschapter 6 in in: V.C. Farmer (Ed.), The infrared spectra of minerals, Mineralogical Society monograph, 4, Mineralogical Society, London, 1974.

[36] C. Ararat–Ibarguen, A. Mosquera, R. Parra, M.S. Castro, J.E. Rodríguez–Páez, Synthesis of SnO_2 nanoparticles through the controlled precipitation route, Mater. Chem. Phys. 101 (2007) 433–440.

[37] C. Fernández–Perdomo, E. Rivera–Figueroa, J.E. Rodríguez–Páez, $BaTiO_3$ obtained by coprecipitation method, Dyna 75 (156) (2008) 223–230.

[38] H.A. Ávila, J.E. Rodríguez-Páez, Solvent effects in the synthesis process of tin oxide, J. Non-Cryst. Solids 355 (2009) 885–890.

[39] M.S. Thompson, G.H. Wiseman, Synthesis and microstructure of gel-derived varistor precursor powders, Ceram. Int. 15 (1989) 281–288.

[40] L.W. Tai, P.A. Lessing, Modified resin-intermediate processing of perovskite powders: Part I. Optimization of polymeric precursors, J. Mater. Res. 7 (2) (1992) 502–510.

[41] M.P. Pechini, U.S. patent No. 3330, 697, july 1967.

[42] D. Hennings, W. Mayr, Thermal decomposition of (BaTi) citrates into barium titanate, J. Solid State Chem. 26 (1978) 329–338.

[43] N.S. Gajbhiye, U. Bhattacharya, V.S. Darshane, Thermal decomposition of zinc–iron citrate precursor, Thermochim. Acta 264 (1995) 219–230.